Extended x-ray-absorption fine-structure study of $Ga_{1-x}In_xAs$ random solid solutions

J. C. Mikkelsen, Jr. and J. B. Boyce
Xerox Palo Alto Research Center, Palo Alto, California 94304
(Received 23 June 1983)

The extended x-ray-absorption fine structure was measured on the K edges of each of the elements in $Ga_{1-x}In_xAs$ solid solutions for x ranging from 0 to 1. The Ga-As and In-As near-neighbor distances remain nearly constant across the solid solution, varying by only 0.04 Å. The *average* cation-anion distance, on the other hand, changes by 0.174 Å. The second-neighbor spectra indicate that the anion (As) sublattice is the more distorted, with two distributions of As-As distances, separated by 0.24 Å. In contrast, the cation (Ga,In) sublattice approximates an average face-centered-cubic lattice, i.e., a virtual crystal, with cation-cation distributions which are peaked within 0.05 Å of the mean. This type of first- and second-near-neighbor environment is similar to that in chalcopyrite with $c/a=2$ and $u=0.270$, rather than that of an average, or virtual, crystal.

I. INTRODUCTION

In principle all materials have a finite solubility in one another, dramatically increasing the possibilities for engineering the materials properties. In very dilute concentrations, for example, dopant impurities in silicon enable the fabrication of integrated circuits. In the concentrated alloy regime, for materials where completely miscible solid solutions are formed, the properties can often be varied continuously between the two endpoints. An example of such a system is a solid-state laser made from $Ga_{1-x}Al_xAs$ or $Pb_{1-x}Sn_xTe$, in which the laser wavelength can be changed by varying x. However, the atomic-scale structure of these and other technologically important electronic materials is insufficiently known to quantitatively predict the effect of a dilute impurity or a substituted constituent atom on either the electrical or thermodynamic properties of the solid solution. For example, thermodynamic modeling of III-V alloys has emphasized solid-liquid equilibria important for crystal growth,[1] with only recent attention placed on the strain-related stability of ternary and quaternary solid solutions.[2]

The structural characterization of alloys originated with the use of x-ray diffraction to measure the lattice constants as a function of composition. However, the Bragg scattering averages over many unit cells, and the extent of atomic displacements from ideal lattice sites is contained in the diffuse background which is generally more difficult to quantitatively obtain and analyze.[3] Vegard[4] noted that the lattice constant of many alloys, determined by Bragg x-ray diffraction, varied linearly with the composition between the end members, suggesting that atomic volume was conserved regardless of the details of the local distortions of the lattice. This is equivalent to saying that the partial molar volume of each constituent is independent of concentration, a situation realized by ideal solutions. It would be anticipated that the "molar bond lengths" would remain constant with composition as well, approximated to first order by the additivity of covalent radii in tetrahedrally coordinated compounds, as suggested by Pauling and Huggins.[5] Many semiconductor ternary solutions have been found to closely approximate Vegard's law, and such is the case for the material of interest here, $Ga_{1-x}In_xAs$.[6]

Although the simple chemical concepts favor the use of approximately constant atomic (ionic or covalent) radii for alloy constituents, one of the most commonly used models for solid solutions is the virtual-crystal approximation[7] (VCA). In this model not only are all the atoms located on ideal lattice sites of the average unit cell, thereby ignoring any local displacements, but also the substituted sublattice, e.g., Ga and In in $Ga_{1-x}In_xAs$, assumes an average value of bond length, bond ionicity, atomic potential, etc. The moderate success of this model in metal or semiconductor band-structure calculations lies in the fact that the electron wave functions of interest are delocalized in the formation of valence and conduction bands, which obscure much of the details of the atomic site potentials. However, it is presently recognized that fluctuations in atomic potentials may contribute to carrier scattering and reduced mobility in semiconductor alloys.[8] Improvements on the VCA have attempted to account for the different potentials on the substituted sublattice. In particular, both a dielectric method[9] and the coherent-potential approximation[10] (CPA) have been used to model the electronic structure of III-V alloys. More recently, the CPA has been applied to the $Hg_{1-x}Cd_xTe$ alloy valence-band structures,[11] determined by photoelectron spectroscopy,[12] in which the difference between Hg-Te and Cd-Te interactions, which are ignored in the VCA, were examined. However, the displacement of isovalent atoms from the ideal lattice sites is not explicitly treated in the CPA models. The VCA is also expected to be a poor model for phenomena which depend strongly on the localized bonding environment, such as nuclear magnetic resonance. Measurement[13] and calculation[14] of the quadrupolar interactions in dilute alkali-halide solid solutions indicated substantial displacement of the anions around an isovalent cation impurity. Although atomic-level probes can be sensitive to the details of the local chemical bonding, it is often difficult to extract the structural information directly from these measurements.

A particular model that yields a structure different from that of the VCA is worth noting in regard to the prototype alloy system we have chosen. Based on a two-dimensional lattice model, Fong, Weber, and Phillips[15] (FWP) proposed that the S-shaped lattice constant deviation from Vegard's law for certain $AC_{1-x}D_x$ zinc-blende alloy systems resulted from a bimodal distribution of cation-anion near-neighbor spacings, centered approximately at the distances in the pure binary end members. Although the bimodal bond-length distribution was attributed to strong bond-bending force constants characteristic of covalently bonded zinc-blende materials, the S-shaped lattice constant behavior occurred when there was a large difference between the bond-bending force constants for the two binary constituents. In any case this model predicts a bimodal near-neighbor bond-length distribution with the bond angles being preserved at the tetrahedral value rather than the single bond-length distribution of VCA.

In contrast to the difficulties presented by analyzing diffuse x-ray scattering, extending x-ray absorption fine structure (EXAFS) is well suited for the determination of near-neighbor spacings,[16] especially relative to a well-defined standard. It provides a direct characterization of the local distortions present in solid solutions. It is somewhat surprising that EXAFS has not been extensively exploited in the study of random alloys. Rather, the issues in alloys that have been addressed using EXAFS have been predominately those of deviations from random substitution, such as the formation of Guinier-Preston zones in Cu_xAl_{1-x},[17] and clustering in spin-glasses.[18,19] However, several dilute, metallic alloy solutions, 3 and 7.3 at. % Mg in Al,[20] 0.8 at % Zn in Al,[21] and 2 at. % Cu in Al (Ref. 17) have been studied by EXAFS, and it was observed that the impurity-host distances were much closer to the sum of metallic radii of the host than the calculated distances based on an elastic continuum model.[22] In these cases the absolute accuracy of the near-neighbor distance determinations was somewhat limited since there were no ideal structural standards with which to compare the unknowns. On the other hand, EXAFS has been used in the study of compound solid solutions, where the end members can be used as the reference structures. We have used EXAFS to study the local bonding environment in the vacancy zinc-blende compound $Ga_{2/3}Se$ and its solid solutions with GaAs.[23] In the EXAFS study of the mixed-valence solid solutions $Sm_{0.75}Y_{0.25}S$ it was found that the Sm-S and Y-S near-neighbor spacings were 2.82 and 2.77 Å, respectively, whereas the lattice constant of 5.66 Å indicates an average near-neighbor spacing of 2.83 Å.[24] Azoulay *et al.*[25] calculated the Pr-Sb distance in $Er_{1-x}Pr_xSb$ alloys containing 5 and 10 mole % Pr from the measured Er-Sb distance assuming the validity of Vegard's law, and found it to be closer to the Pr-Sb distance in PrSb than the Er-Sb distance of the host. This value, however, had a rather large uncertainty (±0.10 Å for the calculated Pr-Sb distance of the 5 mole % alloy) due to the fact that the measured Er-Sb distance and the average near-neighbor distance differs by only 0.009 Å, comparable to the measurement uncertainty. A direct measurement of the Pr-Sb distance should be able to yield a more accurate result.

We show that, with the appropriate choice of known structural standards, EXAFS can be used to determine the local environment in ternary solid solutions with an accuracy of 0.005 Å in near-neighbor distance, and important further-neighbor information with somewhat less accuracy. We chose the $Ga_{1-x}In_xAs$ pseudobinary solutions as a prototype compound alloy system for the following reasons: (1) GaAs and InAs crystallize in the simple zinc-blende structure, space group $F\bar{4}3m$, in which each sublattice is face-centered cubic (fcc) [and the near-neighbor (NN) spacing is equal to $3^{1/2}a_0/4$, where a_0 is the lattice constant]. (2) The difference in the Ga-As and In-As distances of 0.174 Å (2.448 and 2.622 Å in GaAs and InAs, respectively) is the largest among III-V solid solutions and should maximize local distortions arising from cation substitution. (3) A complete solid solution exists with linear lattice constant behavior (which provides a test of the FWP model[15] even in the absence of deviations from Vegard's law). (4) All three elements have readily accessible K-absorption edges for EXAFS analysis. (5) In addition, this model system is of particular interest since it is the subject of recent investigations of carrier scattering due to local potential fluctuations arising from 2% composition fluctuations over 1000-Å clusters.[8] A short paper summarizing our major conclusions from the EXAFS data on $Ga_{1-x}In_xAs$ has already appeared.[26]

II. EXPERIMENTAL DETAILS

A. Sample preparation

Alloys were prepared by quenching melts of appropriate ratios of stoichiometric GaAs and InAs, and the resulting solids were repeatedly ground and sintered until the x-ray diffraction patterns were sharp, i.e., good $K\alpha_1$-$K\alpha_2$ resolution of high-angle diffractions. Examples of the (422) reflections for the end-point compounds and five alloy compositions are shown in Fig. 1. The slightly poorer alloy peak resolution compared to pure GaAs and InAs can arise from either slight variation in composition across the polycrystalline sample due to a slight temperature gra-

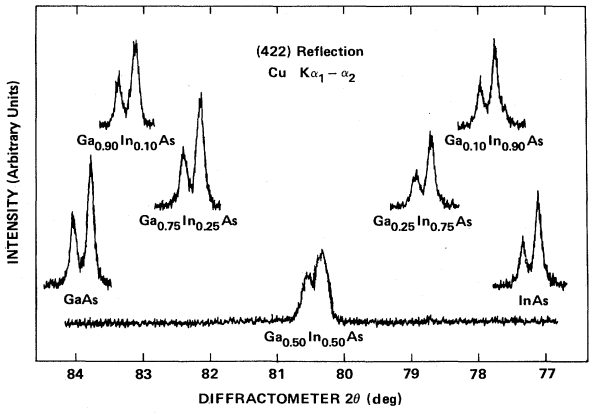

FIG. 1. X-ray (422) diffraction peaks of GaAs, InAs, and five alloy compositions, using Cu $K\alpha_1$-$K\alpha_2$ radiation, indicating that the alloys are chemically homogeneous.

dient during annealing or atomic scale segregation. A detailed examination of the x-ray broadening is beyond the scope of this study and would require a monochromated source and narrow slits to reduce the instrumental broadening. However, it is obvious that the alloys are not composed of a mixture of GaAs- or InAs-like particles. From the maximum observed broadening of approximately 0.003 Å at a d spacing of 1.20 Å for the (422) reflections, compared to a d spacing change from GaAs to InAs of 0.083 Å, we estimate the maximum deviation in composition to be ± 2 mole%, assuming there were discrete, homogeneous particles at least as large as a coherence length, estimated to be ~ 50 Å. Our x-ray results were also used to determine the average lattice constants and we verified that the lattice constant varies linearly throughout the entire solid solution[6] (see Fig. 6 below).

Each EXAFS sample was prepared by mixing a measured amount of ~ 600 mesh powder with epoxy and casting the mixture to obtain a film of optimum optical density, ~ 2.5 absorption lengths. Care was taken to ensure that the samples were of uniform thickness and free of pinholes. This was verified on each sample using x-ray transmission photographs. A second verification was provided by the agreement between the estimated sample thickness and that obtained from the K-edge step height.

B. EXAFS measurements and data reduction

EXAFS measurements were made in transmission at the Stanford Synchrotron Radiation Laboratory using a Si(220) double monochromator crystal on a wiggler beam line. Spectra were taken at 77 K to reduce the Debye-Waller broadening, and at 300 K to reference the low-temperature data to the room-temperature x-ray diffraction data. The details of data collection and analysis have been described elsewhere.[27] An example of the absorption in the vicinity of the Ga K edge in GaAs is shown in Fig. 2(a). The Ga K edge occurs at 10.37 keV and the As K edge is also visible at 11.87 keV. Removal of the background absorption yields the EXAFS, $k\chi(k)$, as a function of photoelectron wave vector, k, shown in Fig. 2(b) for the Ga K edge of GaAs. The large peaks below $k=2$ Å^{-1} are the near-edge structure or white lines. The remaining part of the spectrum is the EXAFS and is described by

$$k\chi(k)\sim\sum_i N_i t_i(k) e^{-2k^2\sigma_i^2} e^{-2r_i/\lambda} \sin[2kr_i+\delta_i(k)]/r_i^2 . \quad (1)$$

The sum is over each shell of neighbors i to the excited atom, $t_i(k)$ is the backscattering matrix for the ith shell, δ_i is the total phase shift experienced by the photoelectron scattered from the ith shell, and λ is the photoelectron mean free path. The photoelectron wave vector k is given by

$$\hbar^2 k^2/2m=(\hbar\omega-E_0) , \quad (2)$$

where $\hbar\omega$ is the incident photon energy and E_0 is the energy threshold of the absorption edge. The structural information is contained in the number of neighbors in each shell N_i, the distance from the excited atom r_i, and the mean-square displacement about the mean, σ_i^2. In isostructural solid solutions we expect that the number of near neighbors, second neighbors, etc., is the same as for the pure binary compounds, ignoring vacancies, interstitials, or antisite defects. The unknown structural parameters in the $Ga_{1-x}In_xAs$ alloys will be the distribution of four Ga and In atoms in the tetrahedron surrounding each As atom, the near-neighbor distances, $r_{\text{Ga-As}}$, $r_{\text{In-As}}$, and further neighbor distances, and their σ_i's.

In order to separate the contribution from widely separated shells of neighbors, the k-space data were Fourier transformed to real space. The real-space spectrum of the excited central atom α, namely $\phi_\alpha(r)$ is given by

$$\phi_\alpha(r)=\sum_\beta \int dr' p_{\alpha\beta}(r')\xi_{\alpha\beta}(r-r')/r'^2 , \quad (3)$$

where $p_{\alpha\beta}(r)$ is the pair correlation function of the β atoms about the excited central atom α. As in Eq. (1), $p_{\alpha\beta}(r)$ is assumed to be a Gaussian, normalized such that $\int dr\, p_{\alpha\beta}(r)=N_\beta$, the number of β atoms at $r_{\alpha\beta}$, that is,

$$p_{\alpha\beta}(r)=\{N_\beta/[(2\pi)^{1/2}\sigma]\}\exp[-(r-r_{\alpha\beta})^2/2\sigma^2] . \quad (4)$$

$\xi_{\alpha\beta}$ is the Fourier transform of those factors that describe the electron scattering process, namely $t(k)$, $e^{-2r/\lambda}$, and

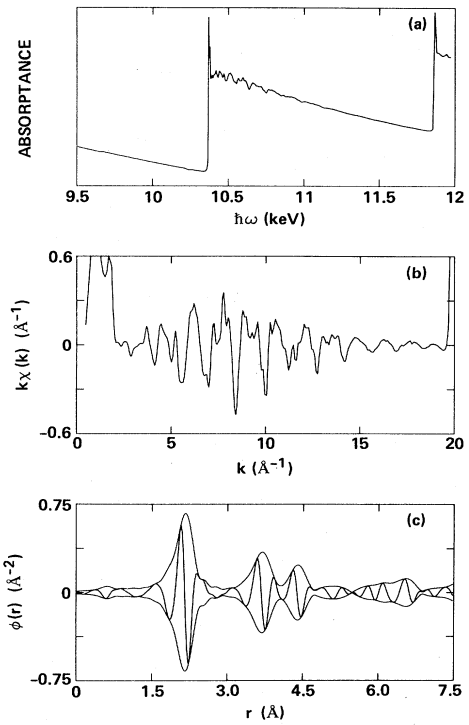

FIG. 2 (a) Absorption as a function of photon energy about the Ga K edge at 10.37 keV in GaAs at 77 K. (b) Ga K-edge EXAFS oscillations, $k\chi(k)$, as a function of k after removal of the background absorption. (c) Fourier transform of (b) to real space. The transform window is 3.76–18 Å^{-1}, broadened by a Gaussian of width 0.7 Å^{-1}.

$e^{i\delta(k)}$. $\xi_{\alpha\beta}$ is obtained from structurally known standards which are chemically similar to the unknown. In this study, the binary compounds GaAs and InAs serve as the structural standards, and we expect that the chemical nature of the alloys varies smoothly between the two compounds. An example of a $\phi(r)$ is shown by Fig. 2(c) for the Ga K-edge data on GaAs. The first peak is due to the four As near neighbors at 2.44 Å, and the second peak is due to 12 Ga second neighbors at 4.00 Å, and so forth.

In the analyses described below, the data for the unknown in real space $\phi(r)$ were compared with model real-space functions, $\phi_m(r)$, constructed using the $\xi(r)$ extracted from the GaAs and InAs standards. All the various pairs of central atom and backscattering atom needed to analyze the data were obtained from these structurally well-known standards, except for the unlike cation-cation signature. These signatures were obtained from the dilute alloys as described below. One- and two-Gaussian models were used for the $p(r)$ of the unknown, and the Gaussian parameters N, r_0, and σ for each Gaussian were adjusted in a least-square fit to the data, minimizing a reliability-of-fit parameter.[27] Unless otherwise indicated, the results described below were obtained from the 77-K data, but the bond lengths are referred to the 300-K x-ray lattice constant measurements of the GaAs and InAs standards. The change in $r_{\text{Ga-As}}$ and $r_{\text{In-As}}$ from 77 to 300 K was +0.004 and +0.001 Å, respectively, and the observed changes in the alloys were within these limits.

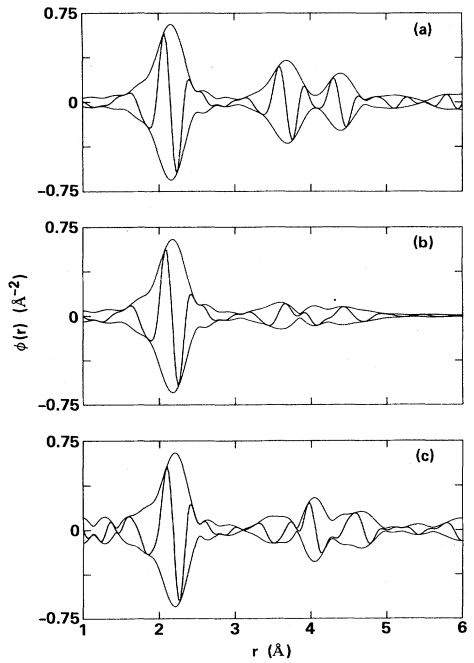

FIG. 3. Ga K-edge EXAFS in real space transformed using a window of $k = 3.56$–15.65 Å^{-1} broadened by a Gaussian of width 0.7 Å^{-1} for (a) pure GaAs, (b) $Ga_{0.5}In_{0.5}As$, and (c) $Ga_{0.1}In_{0.9}As$. Note the similarity of the first-neighbor As peak position, width, and amplitude (i.e., similar r, σ, and N). The second-neighbor peaks, on the other hand, are quite different.

III. RESULTS AND DISCUSSION

A. Near-neighbor environments

1. Ga and In central atom

We have analyzed the Ga and In K-edge EXAFS of seven alloys to determine the change in the Ga-As and In-As bond lengths, $r_{\text{Ga-As}}$ and $r_{\text{In-As}}$, as a function of alloy composition. Representative real-space data for three different compositions are shown in Fig. 3 for the Ga K edge and in Fig. 4 for the In K edge. As a general feature, the first peak in the Ga and In K-edge $\phi(r)$ of the alloys are sharp and similar to those in the respective standards, whereas the second peak is broadened and shows interference. This behavior is due to the fact that the first neighbor to each cation is only As, whereas the second-neighbor shell is mixed (Ga,In). Also it is obvious from Figs. 3 and 4 that the Ga-As and In-As first-neighbor distances in the alloys are quite close to those in the compounds GaAs and InAs, respectively, and not close to those assumed by a virtual crystal. This is confirmed by a detailed least-squares analysis and is readily evident in Fig. 5, which shows the Fourier-filtered EXAFS in k space due to the GaAs first-neighbor peaks. The solid line is that for GaAs, and the dots are for $Ga_{0.1}In_{0.9}As$ shifted by −0.03 Å. The two curves agree in amplitude, i.e., N, in damping, i.e., σ, and in phase, showing that the near-neighbor environment in the two materials is the same with only a small 0.03-Å increase in the Ga-As distance for the alloy. The alloy $r_{\text{Ga-As}}$ and $r_{\text{In-As}}$, adjusted to 300-K x-ray dif-

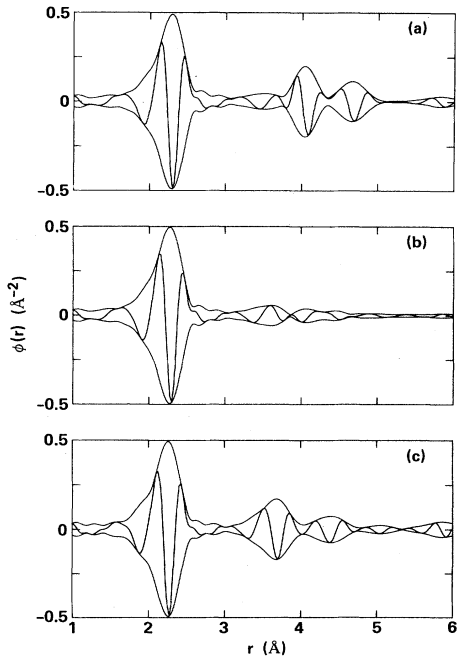

FIG. 4. In K-edge EXAFS in real space transformed using a window of $k = 3.96$–18 Å^{-1} broadened by a Gaussian of width 0.7 Å^{-1} for (a) pure InAs, (b) $In_{0.5}Ga_{0.5}As$, and (c) $In_{0.1}Ga_{0.9}As$, all at 77 K. Note the similarity of the first-neighbor As peak position, width, and amplitude (i.e., similar r, σ, and N). The second-neighbor peaks, on the other hand, are quite different.

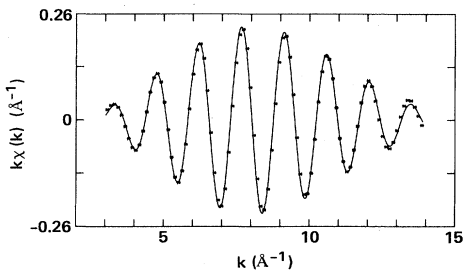

FIG. 5. Fourier filtered EXAFS on the Ga K edge for the first-neighbor peaks in pure GaAs (solid line) and $Ga_{0.1}In_{0.9}As$ (dots). The latter has been shifted in real space by -0.03 Å. The k to r transform range is 3.4—13.8 Å^{-1} broadened by a Gaussian width of 0.5 Å^{-1}. The r to k transform range is 1.8—2.6 Å, i.e., the first-neighbor As peak. The fact that the two curves agree implies that the N and σ of the alloy are the same as that in pure GaAs, but that the near-neighbor spacing is larger in the alloy by the shift of 0.03 Å.

fraction values, are shown by the lower and upper curves, respectively, in Fig. 6. We estimate an uncertainty of 0.005 Å in near-neighbor spacings, corresponding to a factor of 2 increase in the reliability-of-fit parameter from a minimum value, except in the dilute alloys (1—2 mole %) where the error is $\sim$0.01 Å. The total increase in $r_{Ga\text{-}As}$ from pure GaAs to 2 mole % in InAs is 0.044 Å, or $\sim$25% of the difference between $r_{Ga\text{-}As}$ and $r_{In\text{-}As}$ in the end-point compounds. At the same time the $r_{In\text{-}As}$ decreases by the same amount. It is readily apparent that the $r_{Ga\text{-}As}$ and $r_{In\text{-}As}$ differ substantially from the virtual crystal, average cation-anion distance, shown in Fig. 6 by the middle curve calculated from the x-ray diffraction data, which is seen to accurately follow Vegard's law. However, the weighted mean cation-anion NN spacing is

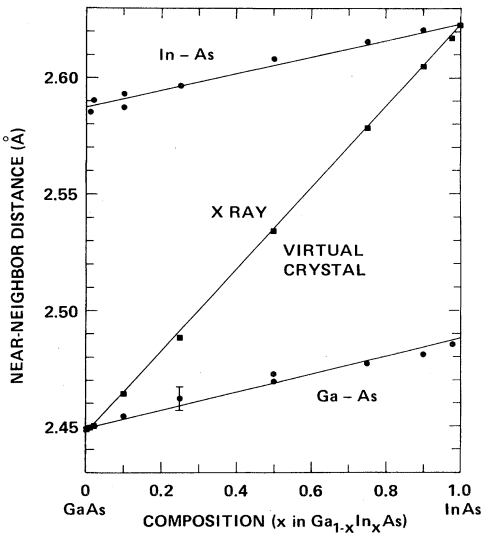

FIG. 6. Ga-As and In-As near-neighbor distances as a function of alloy composition. Middle curve is the VCA cation-anion bond length calculated from the measured x-ray lattice constant. The weighted average of the two NN distances agrees with the VCA (lattice constant) average.

equal to the virtual-crystal distance, as expected. The measured values of $r_{Ga\text{-}As}$ of 2% GaAs in InAs and $r_{In\text{-}As}$ of 1% InAs in GaAs indicate that there is a small, gradual change in NN spacing from dilute to concentrated alloys, with no indication that the impurity atomic volume rapidly approaches that of the host in this composition range.

Since our impurity bond length is compared directly to a well-known standard, and not calculated as in Ref. 25, we are able to see a small, but significant, change in the Ga-As distances from pure GaAs to the dilute alloys, in disagreement with the conclusion of Azoulay *et al.*[25] that the near-neighbor spacings in solid solutions remain *constant.* In $Ga_{1-x}In_xAs$ alloys the change in NN distances is approximately 25% of the average VCA bond-length change. Since this system strictly obeys Vegard's law, the small change in bond lengths is compensated by a change in bond angle in order to maintain a composition-independent molar volume.

The other significant observation is that the width (σ) of the distribution of Ga-As and In-As distances in the alloys is essentially the same as that in GaAs or InAs. This is evident from the data in Figs. 3—5. We estimate that at 77 K the thermal broadening (Debye-Waller factor) contributes $\sim$0.05 Å to the σ in the Ga-As near-neighbor distribution. The widths of the NN distributions in the alloys are the same to within 0.01 Å, i.e., we measure no additional broadening, either from dynamic or static contributions. If the data in Fig. 6 are considered, the narrow near-neighbor distributions are not surprising. The random distribution of Ga and In atoms in the nominal $Ga_{0.5}In_{0.5}As$ alloy will contain atomic-scale fluctuations which appear like $Ga_{0.25}In_{0.75}As$ and $Ga_{0.75}In_{0.25}As$, and so forth. However, the additional contribution to the cation near-neighbor width from these other "local compositions" would be only $\sim$0.02 Å. Our estimated error in determination of σ is of this order, which precludes the use of the cation NN EXAFS analysis to measure the degree of atomic-scale chemical inhomogeneity. This information is available, however, in the cation second-neighbor data discussed below.

2. As central atom

Unlike the cation first-neighbor peak, the first peak in the As K-edge $\phi(r)$ shows interference because the first-neighbor shell is mixed (Ga,In). The Ga and In atoms have only As NN, while the NN environment of each As contains a mixture of Ga and In on the four tetrahedral sites. This is shown in Fig. 7, where, unlike the cation edge data of Figs. 3 and 4, the first-neighbor peaks do differ for the different compositions. However, we have good reference signatures for either Ga or In backscattering from As central atoms in the two standards, GaAs [Fig. 7(a)] and InAs [Fig. 7(c)]. The As K-edge first-neighbor EXAFS were fit by two Gaussian distributions, with the use of the shifted signatures of the standards with either the amplitudes fixed at the ratio of the constituents in the nominal composition or with the amplitudes variable. Both fits gave good results, and in all cases the best fits with variable amplitudes gave within 10% of the

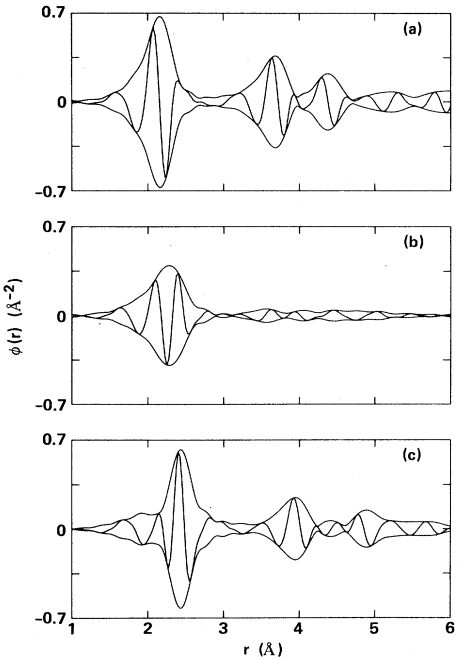

FIG. 7. As K-edge EXAFS in real space transformed using a window of 4.16—17.85 Å^{-1} broadened by a Gaussian of width 0.7 Å^{-1} for (a) pure GaAs, (b) $Ga_{0.5}In_{0.5}As$, and (c) pure InAs, all at 77 K. Note that, unlike the cation first-neighbor peaks of Figs. 3 and 4, the first-neighbor peaks here do differ.

expected number of neighbors for a random alloy; the r_i's agreed within 0.005 Å of those obtained from the Ga and In K-edge data, and the σ's for the two-Gaussian fits were broadened less than 0.01 Å relative to the GaAs and InAs standards, also in agreement with the cation K-edge data. In essence, the As NN results confirm the cation NN results, as they should. We cannot, however, conclude anything about the degree of randomness in the solid solutions from the As-edge results. The amplitude results do not reflect the degree of randomness in the alloys since every As atom contributes to the absorption edge and the *total* number of Ga and In neighbors is invariant regardless of the atomic-scale structure, i.e., whether there is a random occupation of the cation sublattice or a physical mixture of GaAs and InAs.

B. Second-neighbor environment

The structural information attained from the NN analysis, which emphasizes the deviation from VCA by two nearly constant Ga-As and In-As distances, is an adequate description of the NN pair interactions. However, there are alternative ways in which the three-dimensional VCA lattice can distort to accommodate two different cation-anion distances, and further-neighbor information can suggest the nature of this distortion. Unfortunately, the uncertainty in the further-neighbor EXAFS analysis increases for several reasons. First, the contribution to the EXAFS decreases rapidly with distance from the central atom, decreasing the signal-to-noise ratio, as shown in Fig. 2(c). Second, the further-neighbor $\phi(r)$'s are less separated, which means a possible interference between the peaks. Third, in the alloys there will be greater interference between backscattered waves from atoms of different kinds (or at different distances) in the same shell, reducing the sensitivity of the models. And finally, the fits will be at least two Gaussians, with six or more adjustable parameters. Our experience indicates that these parameters are not completely orthogonal, and to attain physical significance, some limited ranges of the parameters, especially the amplitudes, must be used. Nonetheless, good fits were obtained with physically realistic parameters using the analysis procedure described above, although with less precision than for the first neighbors.

1. As-As distribution

In contrast to the mixed-cation NN environment about each As atom, the 12 second neighbors (NNN) are only As atoms, as in the GaAs and InAs standards. A single Gaussian $\phi_m(r)$ derived either from the NNN peak in GaAs or InAs did not give good fits to the As-As peak in the alloys. It is evident from Fig. 7(b) for $Ga_{0.5}In_{0.5}As$ that there is an interference between As-As peaks at different distances, and that two As-As distances are required. Good fits were obtained if two Gaussian peaks were used, one which is derived from As-Ga-As (the smaller $r_{\text{As-As}}$), and the other derived from As-In-As (the larger $r_{\text{As-As}}$), with weighted amplitudes in proportion to their respective mole fractions in the alloy. As expected, good fits were also obtained using *two* appropriately shifted model $\phi_m(r)$'s determined from either GaAs or InAs, indicating that multiple scattering through intervening cations is unimportant. The resulting $r_{\text{As-As}}$'s are plotted versus alloy composition in Fig. 8. Both the $r_{\text{As-As}}$'s are consistent with a small, systematic change with composition that is similar to the 0.044-Å change observed in the NN $r_{\text{Ga-As}}$ and $r_{\text{In-As}}$. The weighted mean of the two $r_{\text{As-As}}$ gives the VCA NNN distance, indicated by the solid line in Fig. 8, as it should. Strictly speaking, within the larger experimental uncertainties for the NNN analysis, the $r_{\text{As-As}}$'s might change even less with composition than $r_{\text{Ga-As}}$ or $r_{\text{In-As}}$.

The σ's for the NNN As-As Gaussian distributions

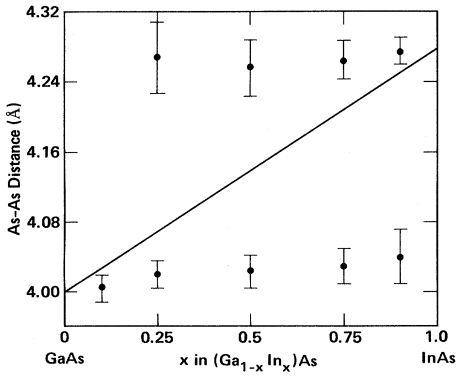

FIG. 8. As-As second-neighbor distances for $Ga_{1-x}In_xAs$ as a function of composition. Two As-As distances are observed, the shorter one corresponding to As—Ga—As bonds and the longer one corresponding to As—In—As bonds. The middle curve is the VCA As-As distance.

were approximately 0.06 Å larger for the dilute alloys, and up to 0.08 Å larger for the 50:50 alloy, than in the GaAs and InAs standards. The separation between the maxima is 0.24 Å, nearly three times each width. It is for this reason that a single, broadened Gaussian distribution gave a poor fit to the data. Although the As-As distribution is highly correlated to the identity of the intervening cation, the additional width is reasonable if it is recognized that each As atom has bonds to three other cations, which also affect its position. It is apparent that the As sublattice strongly deviates from a virtual crystal. Therefore, the alloy structure cannot be described by a regular fcc anion sublattice with the Ga and In atoms occupying off-lattice sites to reflect their respective covalent radii.

2. (Ga,In)-(Ga,In) distribution

The analysis of the cation NNN EXAFS is complicated by the lack of a structural standard from which to derive the mixed cation $\xi_{\text{Ga-In}}$ and $\xi_{\text{In-Ga}}$. For the Ga-edge data, for example, the NNN will be a mixture of Ga and In in proportion to the alloy composition in the absence of segregation. This mixture of atoms in the same shell causes an interference, which can be readily seen in the $\phi(r)$ shown in Fig. 3. The NNN peak occurs at 3.4—4.1 Å, and although it is observed in pure GaAs (which has only Ga in the second-neighbor shell), Fig. 3(a), it is much reduced in the 50:50 alloy, Fig. 3(b), by this interference.

In order to model the NNN EXAFS the $\xi_{\text{Ga-Ga}}$ can be readily obtained from GaAs. In order to derive a simulated $\xi_{\text{Ga-In}}$, we used the 10% GaAs in InAs, in which on the average 90% of each Ga atom's 12 second neighbors should be In atoms. This procedure will be in serious error if there is measurable segregation, that is, fewer than the statistical average number of In atoms about each Ga. Similarly, the In-edge EXAFS on the $Ga_{0.9}In_{0.1}As$ alloy was used to derive $\xi_{\text{In-Ga}}$. The Ga-In (or In-Ga) distance is unknown *a priori* so distances of 4.23 and 4.05 Å for the $r_{\text{In-Ga}}$ and $r_{\text{Ga-In}}$ in the 10 and 90 mole% GaAs alloys, respectively, were used. These values are within 0.02 Å of the respective VCA values of 4.25 and 4.02 Å, and were obtained by minimizing the difference between $r_{\text{Ga-In}}$ and $r_{\text{In-Ga}}$ obtained separately from the Ga- and In-edge EXAFS in the same alloy. The results of the cation NNN analysis for the 75, 50, and 25 mole% GaAs alloys are plotted in Fig. 9. Also included are the $r_{\text{Ga-In}}$ used for the 90% and 10% alloy standards used to simulate $\xi_{\text{Ga-In}}$ and $\xi_{\text{In-Ga}}$. The $r_{\text{Ga-Ga}}$ and $r_{\text{In-In}}$ differ by $\sim$0.08 Å, and the adjusted $r_{\text{Ga-In}}$ and $r_{\text{In-Ga}}$ agree to within 0.01 Å. The weighted mean of these various distances is very close to the VCA average distance (solid line). Despite the fact that the precise cation-cation distribution is difficult to obtain from EXAFS because of the uncertainties in the mixed-cation signature in addition to the usual uncertainty associated with second neighbors and two-Gaussian fits noted above, the general features are clear. The qualitative distinction between the cation and anion sublattice is inescapable. The Ga-Ga, Ga-In, and In-In are all within $\sim$0.05 Å of the VCA cation-cation distance, whereas the As-As distances are bimodal. We thus conclude that the mixed-cation sublattice more closely approximates a virtual crystal than the common-anion sublattice. All of these second-neighbor bond-length distributions have an additional 0.04—0.08 Å broadening compared to the pure compound standards. This additional broadening probably reflects the static distribution of bond lengths characteristic of the fluctuations in the local composition about the nominal average.

The NNN cation EXAFS results can be used to qualitatively characterize the degree of randomness in these solid solutions. It is obvious in Figs. 3(a) and 3(b) that the Ga NNN environment is very different for GaAs and the 50:50 alloy [and correspondingly, in Fig. 4(a) and 4(b) for the In NNN environment in InAs and the 50:50 alloy]. If small GaAs- and InAs-like particles existed, Ga and In atoms would have predominantly *like* NNN, i.e., Ga or In NNN, respectively. Our detailed fits yield the result that both elements have nearly the expected mixture of Ga and In NNN corresponding to the alloy composition. In particular the dilute alloys provide the most sensitive test for clustering. In $Ga_{0.1}In_{0.9}As$ the Ga atoms would have 10% Ga NNN and 90% In NNN if the alloy were randomly mixed, but a larger concentration of Ga neighbors if there were microclusters. We obtain 10% Ga and 90% In NNN for this alloy. We thus have the first experimental evidence that appreciable clustering on the atomic scale is absent in this zinc-blende solid solution. The second observation pertains to the widths of the mixed-cation distributions. For example, in the 50:50 alloy, the $r_{\text{Ga-Ga}}$ distribution is centered at 4.10 Å, with a σ of 0.08 Å greater than that in pure GaAs. We presume that most of the additional σ results from a static fluctuation in $r_{\text{Ga-Ga}}$ due to chemical fluctuations, i.e., a distribution of $AsGa_xIn_{4-x}$ tetrahedra which leads to the variations in the Ga-Ga distances. A quantitative model of NNN bond-length distributions requires specifying the atomic positions of at least four shells beyond the central atom.[28] However, since the amplitude of the Ga-Ga distribution at the $r_{\text{Ga-Ga}}$ of GaAs (4.00 Å) is less than half the peak amplitude of the 50:50 alloy at 4.10 Å, we conclude that most of the cation-cation distribution comes from $AsGa_3In$, $AsGa_2In_2$, and $AsIn_3Ga$ tetrahedra, as expected from random cation arrangements.

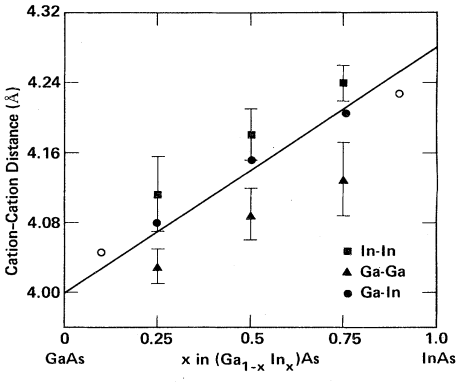

FIG. 9. Ga-Ga, In-In, and Ga-In second-neighbor distances for 25, 50, and 75 mole% GaAs. The values of In-Ga and Ga-In distances obtained from the 90 and 10 mole% alloys, as explained in the text, are indicated by (○). The cation-cation distances are seen to approach the VCA values, the solid line.

Finally, cluster parameters have been calculated from a model for the infrared reflectivity of several III-V alloys.[29] The maximum clustering was obtained at $Ga_{0.5}In_{0.5}As$, with a ratio of Ga-Ga to Ga-In (or In-In to In-Ga) pairs equal to 1.5, corresponding to 7.2 Ga and 4.8 In second neighbors to a Ga, rather than the random values of 6 and 6, a 20% deviation. The clustering parameter reduced to zero below 15 mole% InAs and above 80 mole% InAs. If this second conclusion is correct, then our use of the 10 and 90 mole% alloys as random alloy standards for $r_{Ga\text{-}In}$ and $r_{In\text{-}Ga}$ is on firm ground. However, a 20% deviation from randomness for the 50:50 alloy seems a bit large. Our error bars on the amplitudes of the two Gaussians used to fit the second-neighbor EXAFS is about 15%, so we could not distinguish between a completely random alloy and a slight clustering of about 10%.

C. Chalcopyrite model for pseudobinary alloys

How then does the crystal accommodate the random mixing of a sublattice with two distinctly different cation-anion distances, two anion-anion distributions, and a nearly single, average cation-cation distribution? The ternary, zinc-blende-related, chalcopyrite crystal structure is a close approximation to these bonding constraints. $CdGeAs_2$, for example, could be considered isoelectronic with $InGaAs_2$ ($Ga_{0.5}In_{0.5}As$ alloy), except that the Cd and Ge atoms occupy the cation sites in an ordered distribution, as shown in Fig. 10. The cation ordering produces a new unit cell which is doubled in one direction, defining the c axis, while it retains the a axis of approximately the original zinc-blende lattice constant. The cation ordering in $CdGeAs_2$ results in every tetrahedron surrounding each anion to be identical, i.e., each As is surrounded by 2 Cd and 2 Ge. In the pseudochalcopyrite model for $InGaAs_2$, each As would be surrounded by 2 Ga and 2 In. The ordering of the cations in the chalcopyrite structure results in a second deviation from the zinc-blende crystal structure. The c axis is generally less than twice the a axis, known as the tetragonal compression. In this general case the cations occupy face-centered *tetragonal,* rather than *cubic,* lattice positions. However, in the case of $ZnSnAs_2$ $c/a=2.00$, and the Zn and Sn atoms occupy an fcc sublattice. [$ZnSnAs_2$ also has a zinc-blende polymorph above 670°C (Ref. 30) in which the Zn and Sn atoms are randomly distributed on the cation sublattice.] Since the Ga and In atoms do not order in $Ga_{1-x}In_xAs$ alloys, but retain a cubic rather than tetragonal lattice, we will confine further modeling of the alloy structures to $c/a=2$. We emphasize that this constraint produces an fcc cation sublattice, i.e., it conforms to the virtual-crystal approximation for this sublattice, as observed experimentally.

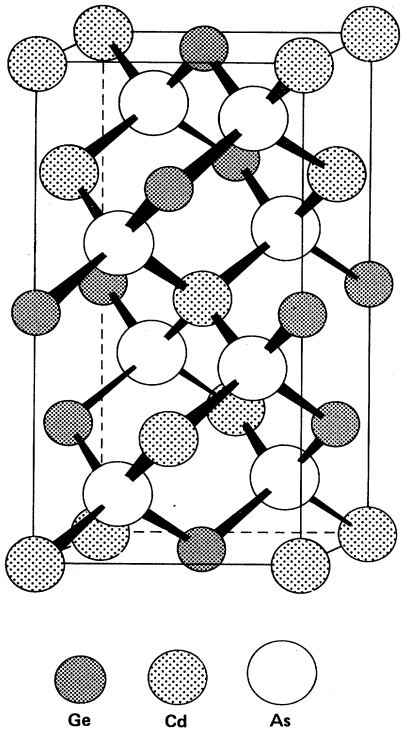

FIG. 10. Schematic of the chalcopyrite crystal structure for $CdGeAs_2$. In the $Ga_{0.5}In_{0.5}As$ alloy the Ga and In atoms have covalent radii which are similar to those of Ge and Cd, respectively. However, no cation ordering is expected in the alloy.

The generalized chalcopyrite structure has a third deviation from the zinc-blende structure, which consists of the anions being displaced from their respective fcc sublattice along (100) or (010) directions. This displacement is defined by a single parameter u which is 0.25 for no displacement from fcc. The anion displacement results in two different cation-anion distances, regardless of the value of c/a. For example, in $CdGeAs_2$, where $c/a=1.889$ and $u=0.285$,[31] all the Cd-As distances are 2.654 Å, and all the Ge-As distances are 2.410 Å. These distances are close to the cation-anion distances observed in $InGaAs_2$. Since c/a is not 2 in $CdGeAs_2$, there are two Cd-Ge distances, one at 4.087 Å, equal to the Cd-Cd and Ge-Ge distances, and the other at 4.202 Å, which corresponds to neighbors in the x-y plane. The tetragonal distortion also leads to eight As-As NNN distances, which reduce to four for $c/a=2$, a value which might be more appropriate for modeling $InGaAs_2$. We next construct a hypothetical chalcopyrite analog to $InGaAs_2$, with $c/a=2$, with the Ga and In atoms occupying the ordered cation positions, and with each As bonded to 2 Ga and 2 In. Of course we have no long-range cation ordering in the alloys, but the local distortions are easier to compute from the atomic position parameters which characterize the ordered chalcopyrite structure.

Perhaps the simplest way to choose the pseudochalcopyrite unit cell to model $InGaAs_2$ is to take a_0 equal to our experimentally measured lattice constant for $Ga_{0.5}In_{0.5}As$, 5.854 Å, and c_0 equal to $2a_0$, 11.709 Å (the slightly smaller cell chosen in Ref. 26 was based on a smaller reported lattice constant for InAs). The best fit to all our experimental first- and second-neighbor distances in $Ga_{0.5}In_{0.5}As$ was obtained with a u parameter of 0.270 [rather than the value of 0.267 (Ref. 26) computed from the deviation of a Ga—As—Ga bond angle from 109.5°]. The calculated $r_{Ga\text{-}As}$ and $r_{In\text{-}As}$ are 2.470 and 2.605 Å, respectively, in good agreement with the EXAFS measured values of 2.466 and 2.610 Å. The calculated $r_{Ga\text{-}Ga}$,

$r_{Ga\text{-}In}$, and $r_{In\text{-}In}$ are all 4.140 Å, determined by the choice of a and c, in necessary agreement with the mean measured values. The $r_{As\text{-}As}$ are a weighted distribution of 2 each at 3.978 and 4.309 Å, and 4 each at 4.060 and 4.225 Å. If this distribution is considered bimodal and peaked at the weighted means of 4.033 and 4.253 Å, there is good agreement with the two measured EXAFS value of $r_{As\text{-}As}$ of 4.02 and 4.26 Å. We thus find good agreement, not only with the two cation-anion NN distances, but also with the NNN bimodal anion-anion and approximately VCA cation-cation distributions as well. We assume that the NN and NNN distributions will be slightly modified when the ordered cation distribution is disordered, and the Ga_2In_2 tetrahedra are replaced by a distribution of Ga_4, Ga_3In, Ga_2In_2, $GaIn_3$, and In_4 tetrahedra, but it is beyond the scope of the present study to quantitatively model the disordered phase. We assume that the Ga-rich tetrahedra will lead to smaller $r_{Ga\text{-}Ga}$, and In-rich tetrahedra will lead to larger $r_{In\text{-}In}$ than the VCA values, in agreement with the larger peak widths obtained from the EXAFS data. We postulate that the other $Ga_{1-x}In_xAs$ compositions accomodate the two cation-anion distances in a similar way, each with distributions of local bonding configurations rather than the ordered cation distribution in the chalcopyrite structure.

Alternatively, the pseudochalcopyrite u parameter can be calculated from the expressions[32] for the near-neighbor bond length as a function of a, c, and u, using our measured values of the 50:50 alloy NN bond lengths. Jaffe and Zunger[33] have extended this chalcopyrite model to predict the "effective" u parameter for ternary III-V alloys where no experimental bond lengths have been measured, assuming that the NN distances are the same as in the pure binary compounds, and predicted the effect of this distortion on the alloy electronic band structure. In their picture it is thus possible to estimate the degree of local atomic distortions knowing only the near-neighbor distances in the end members. The most instructive use of the pseudochalcopyrite model is to recognize that it provides a realistic way for the crystal structure to accommodate what otherwise appear to be unusual constraints.

To the extent that the Ga and In atoms are not on VCA sites, i.e., the $r_{Ga\text{-}Ga}$, $r_{Ga\text{-}In}$, and $r_{In\text{-}In}$ are not quite equal, there may be local distortions similar to those leading to the tetragonal compression found in chalcopyrite, even though cation disorder maintains overall cubic symmetry. Regardless of the model one chooses for representing the local bonding in the $Ga_{1-x}In_xAs$ alloys, the EXAFS results on the NN and NNN distances can be used to determine the three-atom bond angles from the NN and NNN bond lengths. In the 50:50 alloy the Ga—As—Ga and In—As—In bond angles are $112.1\pm1°$ and $106.4\pm1°$, respectively. The double-peaked distributions of bond angles is contrary to the FWP model[15] which has a single distribution of bond angles but a bimodal distribution of bond lengths. The distortion of the VCA lattice to retain NN bond lengths which are within 0.02 Å of those occurring in the pure binary compounds (a 0.8% change) also produces a 2.5% change in bond angle. This partitioning of the distortion is in qualitative agreement with the ratios of the bond-stretching to bond-bending force constants, α/β, of approximately 5 in zinc-blende crystals.[34] Since it cost more energy for a relative change in the bond lengths compared with the bond angle, the stable minimum energy of the crystal results from this partitioning of the local distortion.

D. Alloy models

We first consider the virtual-crystal approximation. To estimate the effect of our measured structural distortions from an average crystal on the electronic band energies, we again turn to the chalcopyrite model of the 50:50 alloy. Of the three chalcopyrite deviations from the zinc-blende structure, the greatest effect on the band structure of $ZnSiAs_2$ is caused by the crystal-field splitting of -0.16 eV arising from the tetragonal compression, whereas the effect of the u parameter was calculated to be a 0.05-eV shift in the valence-band energy at the Γ point.[35] Analogously, we estimate that the effect of local deviations from VCA will contribute a comparable amount to the "bowing" of the alloy bandgaps. Porod *et al.*[36] have parametrized the deviation in the bowing of the band gap from the VCA in III-V alloys by adding an explicit potential term in the Hamiltonian for the unlike cation-cation (Ga-In) interactions which is missing from the VCA. However, this calculation still ignores the structural distortions from VCA which we have observed, and it would appear that the agreement between their model and experiment is fortuitous. Jaffe and Zunger[33] have recently shown that a chalcopyrite-like structural distortion from VCA does in fact contribute substantially (0.17 eV) to the total bowing parameter of 0.50 eV in $Ga_{0.5}In_{0.5}P$.

We next examine the FWP two-dimensional solid solution model[15] derived specifically for zinc-blende alloys, which are characterized by strong bond-bending force constants, to explain the S-shaped deviation of alloy lattice constant from Vegard's law. This model predicts a bimodal NN distribution, each peak broadened and centered about the distance observed in the respective binary compounds. We find that, in $Ga_{1-x}In_xAs$, in which Vegard's law is strictly followed, there is a bimodal distribution of NN distances, but the bimodal distribution of distances is *not* broadened. The FWP model also predicts an S-shaped lattice constant behavior in AC_xD_{1-x} alloys for which the normalized difference in end-member bond-bending force constants, $(\beta_{A\text{-}C}-\beta_{A\text{-}D})/(\beta_{A\text{-}C}+\beta_{A\text{-}D})$, exceeds 0.071. In $Ga_{1-x}In_xAs$ this parameter is 0.24, three times the critical ratio, and yet no S-shaped variation in the lattice constant is observed. To the extent that the strong bond-bending force constants resist the angular distortion, a greater change in bondlength, i.e., a *closer* approach to VCA, will result. The relative extent of central or angular distortion is given by the ratio of central to noncentral force constants, and should be similar for all pseudobinary III-V alloys. If an alloy system exhibits a deviation from Vegard's law, the crystal is unable to achieve a minimum total energy by partitioning the atomic-scale distortions within the limits of a virtual-crystal volume. Although the bimodal bond-length distribution is a correct outcome of the FWP model, the details of the real alloy structure are not obtained from the two-

dimensional model. We also have experimental evidence that the bimodal bond-length distribution is not limited to covalently bonded material, but is observed in the ionicly bonded alkali-halide solid solutions,[37] which also accurately follow Vegard's law. In the ionic solid solutions the total energy of the solid solution is probably minimized by competition between achieving hard-sphere interatomic distances (maximum deviation from VCA) and reducing the electrostatic dipolar energy (minimized at VCA).

There have been several thermodynamic analyses of the solidus-liquidus relations of $Ga_{1-x}In_xAs$ solutions. Foster and Woods[38] modeled the deviations from ideality in the solid solution, and they found that the deviation was only 20% of the strain energy of 2.62 kcal/mole for the 50:50 composition, calculated using an elastic model. Stringfellow and Green[39] determined that the deviations from ideality in *both* the liquid and solid $Ga_{1-x}In_xAs$ solutions were comparable, and it would appear very unlikely that the deviation in the liquid would also arise from a strain term. Stringfellow has recently calculated the stability temperatures for III-V ternary and quaternary solid solutions,[2] and found that a critical temperature of 729 K for the 50:50 alloy was reduced to 0 K when a coherency strain energy term was included, which stabilizes the alloys against composition fluctuations. We are presently using our EXAFS structural information on $Ga_{1-x}In_xAs$ solid solutions to estimate the amount of strain energy arising from two different cation radii.

A more recent attempt to use an elastic model for the structure of random alloys was made by Froyen and Herring,[40] who used a discrete lattice model. Their calculations led to results similar to those obtained by Raoux *et al.*,[20] using an elastic continuum model,[22] namely, that the impurity-host distance, in Cu-Al is predicted to be 2.82 Å, only slightly smaller (by 0.04 Å) than the host (Al-Al) distance. However, there are two conflicting experimental EXAFS measurements of the Cu-Al distance, one which concludes that the Cu-Al distance is 2.79 Å (Ref. 41) and the other a value of 2.725 Å.[17] This latter value is close to the sum of Cu and Al atomic radii, 2.71 Å. Our results on the $Ga_{1-x}In_xAs$ alloy system indicate a behavior which is very similar to the results[17] giving a value of impurity-host distance close to the sum of the atomic radii and quite different from the host-host distance. However, one might expect the structural changes upon alloying to be much different for the covalently bonded zinc-blende compounds than for the metallic Al-Cu system. Nonetheless, the near-neighbor Ga-As and In-As distances remain relatively unchanged in the alloy as a function of composition in analogy with the chemical concept of conservation of atomic radius.

IV. CONCLUSIONS

From EXAFS measurements on the K edges of each of the three elements in $Ga_{1-x}In_xAs$ for x ranging from 0 to 1, we conclude the following: (1) The alloys are close to random at the atomic scale. (2) A significant deviation from VCA exists in the near-neighbor cation-anion distances, which vary only slightly with composition. The near-neighbor Ga-As and In-As distances change by only 0.044 Å, whereas the *average* near-neighbor distance changes by 0.174 Å for x ranging from 0 to 1. (3) The second-neighbor results indicate that the cation-cation distances are approximately equal to the average distance. The anion-anion distribution, on the other hand, is bimodal with As-Ga-As and As-In-As distances close to those in pure GaAs and InAs, respectively. The cation-cation distances approach those of VCA, but the anion-anion distances do not. (4) The local bonding observed in $Ga_{1-x}In_xAs$ is similar to that found in the chalcopyrite structure, so a chalcopyrite analog is proposed to assist in further modeling of the random zinc-blende solid solutions. For the 50:50 composition we obtained the observed first- and second-neighbor distributions with the chalcopyrite parameters of $c/a=2$ and $u=0.270$.

ACKNOWLEDGMENT

The Stanford Synchrotron Radiation Laboratory is supported by the National Science Foundation through the Division of Materials Research.

[1]M. B. Panish and M. Ilegems, in *Progress in Solid State Chemistry,* edited by A. Reiss and J. O. McCaldin (Pergamon, New York, 1972), Vol. 7, pp. 39—84.
[2]G. B. Stringfellow, J. Electron. Mater. 11, 903 (1982).
[3]H. Schulz, in *Current Topics in Material Science,* edited by E. Kaldis (North-Holland, Amsterdam, 1982), Vol. 8, pp. 275—380.
[4]L. Vegard, Z. Phys. 5, 17 (1921).
[5]L. Pauling and M. L. Huggins, Z. Kristallogr. Kristallgeom. Krystallphys. Kristallchem. 87, 205 (1934).
[6]J. C. Wooley and B. C. Smith, Proc. Phys. Soc. London 72, 241 (1958).
[7]L. Nordheim, Ann. Phys. (Leipz.) 9, 607 (1931); 641 (1931).
[8]J. H. Marsh, Appl. Phys. Lett. 41, 732 (1982).
[9]J. A. Van Vechten and T. K. Bergstresser, Phys. Rev. B 1, 3351 (1970).
[10]A. B. Chen and A. Sher, Phys. Rev. B 23, 5360 (1981).
[11]A. B. Chen and A. Sher, J. Vac. Sci. Technol. 21, 138 (1982).
[12]J. A. Silberman, P. Morgan, I. Landau, W. E. Spicer, and J. A. Wilson, J. Vac. Sci. Technol. 21, 142 (1982).
[13]Y. Fukai, J. Phys. Soc. Jpn. 18, 1412 (1963).
[14]B. G. Dick and T. P. Das, Phys. Rev. 127, 1053 (1962).
[15]C. Y. Fong, W. Weber, and J. C. Phillips, Phys. Rev. B 12, 5387 (1976).
[16]T. M. Hayes and J. B. Boyce, in *Solid State Physics,* edited by H. Ehrenreich, F. Seitz, and D. Turnbull (Academic, New York, 1982), Vol. 37, pp. 173—351.
[17]A. Fontaine, P. Lagarde, A. Naudon, D. Raoux, and D. Spanjaard, Philos. Mag. B 4, 17 (1979).
[18]T. M. Hayes, J. W. Allen, J. B. Boyce, and J. J. Hauser, Phys. Rev. B 22, 4503 (1980).
[19]J. B. Boyce and K. Baberschke, Solid State Commun. 39, 781 (1981).
[20]D. Raoux, A. Fontaine, P. Lagarde, and A. Sadoc, Phys. Rev.

B 24, 5547 (1981).
[21]J. Mimault, A. Fontaine, P. Lagarde, D. Raoux, A. Sadoc, and D. Spanjaard, J. Phys. F 11, 1311 (1981).
[22]J. D. Eshelby, in *Solid State Physics,* edited by F. Seitz and D. Turnbull (Academic, New York, 1956), Vol. 3, pp. 79—145.
[23]J. C. Mikkelsen, Jr. and J. B. Boyce, Phys. Rev. B 24, 5999 (1981).
[24]J. B. Boyce, R. M. Martin, J. W. Allen, and F. Holtzberg, in *Valence Fluctuations in Solids,* edited by L. M. Falicov, W. Hanks, and M. B. Maple (North-Holland, Amsterdam, 1981), p. 427.
[25]J. Azoulay, E. A. Stern, D. Shaltiel, and A. Grayevski, Phys. Rev. B 25, 5627 (1982).
[26]J. C. Mikkelsen, Jr. and J. B. Boyce, Phys. Rev. Lett. 49, 1412 (1982).
[27]J. B. Boyce, T. M. Hayes, and J. C. Mikkelsen, Jr., Phys. Rev. B 23, 2876 (1981).
[28]L. Guttman (private communication).
[29]S. Yamazaki, M. Kishi, and T. Katoda, Phys. Status Solidi B 113, 421 (1982).
[30]D. B. Gasson, P. J. Holmes, I. C. Jennings, B. R. Marathe, and J. E. Parrott, J. Phys. Chem. Solids 12, 1291 (1962).
[31]R. W. G. Wyckoff, *Crystal Structures* (Interscience, New York, 1964), Vol. 2, p. 338.
[32]J. L. Shay and J. H. Wernick, *Ternary Chalcopyrite Semiconductors: Growth, Electronic Properties, and Applications* (Pergamon, Oxford, 1975), p. 8.
[33]A. Zunger and J. E. Jaffe, Phys. Rev. Lett. 51, 662 (1983).
[34]R. M. Martin, Phys. Rev. B 1, 4005 (1970).
[35]J. E. Rowe and J. L. Shay, Phys. Rev. B 3, 451 (1971).
[36]W. Porod, D. K. Ferry, and K. A. Jones, J. Vac. Sci. Technol. 21, 965 (1982).
[37]J. B. Boyce and J. C. Mikkelsen, Jr., Bull. Am. Phys. Soc. 28, 490 (1983).
[38]L. M. Foster and J. F. Woods, J. Electrochem. Soc. 118, 1175 (1971).
[39]G. B. Stringfellow and P. E. Green, J. Phys. Chem. Solids 30, 1779 (1969).
[40]S. Froyen and C. Herring, J. Appl. Phys. 52, 7165 (1981).
[41]B. Lengeler and P. Eisenberger, Phys. Rev. B 21, 4507 (1980).